0090-9556/10/3809-1443–1448$20.00
DRUG METABOLISM AND DISPOSITION
Vol. 38, No. 9
34199/3616119
DMD 38:1443–1448, 2010
Printed in U.S.A.

The Dipeptidyl Peptidase-4 Inhibitor Linagliptin Exhibits Time- and Dose-Dependent Localization in Kidney, Liver, and Intestine after Intravenous Dosing: Results from High Resolution Autoradiography in Rats

Andreas Greischel, Rudolf Binder, and Juergen Baierl

Drug Metabolism and Pharmacokinetics, Boehringer Ingelheim GmbH & Co. KG, Biberach an der Riss, Germany

Received April 29, 2010; accepted June 10, 2010

ABSTRACT:

Linagliptin is an orally active dipeptidyl peptidase-4 (DPP-4) inhibitor that is under development for the treatment of type 2 diabetes and shows dose-dependent pharmacokinetics in rats and humans. With microscopic autoradiography, the dose dependence of cellular distribution of [^{3}H]linagliptin-related radioactivity was investigated in kidney at 3 h after intravenous injection of 7.4, 100, and 2000 μg/kg [^{3}H]linagliptin. Furthermore, distribution of radioactivity in kidney, liver, and small intestine was investigated in relation to time (2 min, 3 h, and 192 h) after intravenous injection of 7.4 μg/kg [^{3}H]linagliptin. The localization of radioactivity in the kidney at 3 h after administration of 7.4, 100, and 2000 μg/kg [^{3}H]linagliptin changed with increasing dose from cortical glomeruli and parts of proximal tubule parts to parts of medullar proximal tubule. In addition, the compound distribution in the kidney shifted with time after administration of 7.4 μg/kg [^{3}H]linagliptin from glomeruli (2 min) to the lower parts of proximal tubules (192 h). The radioactivity within proximal tubules was located primarily in the brush border. In the liver, the radioactivity persisted mainly around the portal triads and in the bile duct from 2 min to 192 h. In the small intestine, the radioactivity shifted from the lamina propria (2 min) to the surface of the villi and/or intestinal lumen (192 h). In conclusion, the cellular distribution pattern of [^{3}H]linagliptin-related radioactivity reflected the known distribution of DPP-4. Together with the persistence of binding, this result supports the high relevance of DPP-4 binding of linagliptin for its pharmacokinetics and pharmacodynamics.

Introduction

The incretin hormone glucagon-like peptide-1 (GLP-1) is released by the intestine in response to meals and potentiates glucose-induced insulin secretion. GLP-1 is rapidly degraded in the body by dipeptidyl peptidase-4 (DPP-4); thus, inhibition of this enzyme increases GLP-1 exposure and thereby its effect on the pancreas. Because of this effect, DPP-4 inhibitors are used successfully as oral antidiabetes drugs. Linagliptin is a potent inhibitor of DPP-4, currently in phase III clinical development for the treatment of type 2 diabetes (Eckhardt et al., 2008; Deacon and Holst, 2010). In rats as well as in humans, linagliptin exhibits nonlinear pharmacokinetics and shows concentration-dependent plasma protein binding to its target DPP-4 (Fuchs et al., 2009b; Heise et al., 2009; Retlich et al., 2009).

Although DPP-4 circulates as a soluble enzyme (Mentlein, 1999; Lambeir et al., 2003), the major fraction of total body DPP-4 is not localized in plasma but in peripheral tissues in a membrane-bound form (Fukasawa et al., 1981; Hartel et al.,1988a; Lambeir et al., 2003). A particularly high expression of DPP-4 occurs in the kidney, where the enzyme is localized to the glomerular basement membrane and the proximal convoluted tubules (Kettmann et al., 1992). DPP-4 is also widely distributed in other tissues throughout the body, for example, in epithelial cells of the pancreatic duct, in activated T-helper lymphocytes, in macrophages, and in the skin. As reviewed by Mentlein (1999), the DPP-4 activity per gram of tissue is highest in the kidney, followed by the lung, adrenal gland, jejunum, liver, parotid gland, spleen, and testis.

During investigations on the tissue distribution of linagliptin in wild-type and DPP-4-deficient rats at different dose levels, we found that the gross tissue distribution of linagliptin in rats is affected by saturable binding to its target DPP-4 in tissues, which is probably of high affinity and thus leads to long persistence of a minor portion of the dose in the body (Fuchs et al., 2009a). The highest linagliptin concentrations were detected in the excretory organs, and this might also affect the elimination of linagliptin. Therefore, the aim of the present study was to further investigate the localization of linagliptin on a cellular level in the excretory organs kidney (via urine), liver (via bile), and small intestine (via P-glycoprotein secretion) after intravenous administration of different dosages of [^{3}H]linagliptin to male albino rats using microscopic autoradiography.

Materials and Methods

Test Compound. Radiolabeled [^{3}H]linagliptin (8-(3-(*R*)-aminopiperidin-1-yl)-7-but-2-ynyl-3-methyl-1-(4-methyl-quinazolin-2-ylmethyl)-3,7-dihydropurine-2,6-dione) (Eckhardt et al., 2008) with a radiochemical purity of >97% and a specific radioactivity of 3145 MBq/μmol was obtained from RC TRITEC AG (Teufen, Switzerland). Nonlabeled lina-

This work was sponsored by Boehringer Ingelheim Pharma GmbH & Co. KG, Germany.

Article, publication date, and citation information can be found at http://dmd.aspetjournals.org.

doi:10.1124/dmd.110.034199.

ABBREVIATIONS: GLP-1, glucagon-like peptide-1; DPP-4, dipeptidyl peptidase-4.

gliptin with a purity of 98% was supplied by Boehringer Ingelheim Pharma GmbH and Co. KG (Biberach, Germany).

Photosensitive Emulsion-Coated Slides. Cleaned microscope slides were coated with a photosensitive emulsion LM-1 (GE Healthcare, Little Chalfont, Buckinghamshire, UK). The emulsion contains silver halide crystals with an average diameter of 0.2 μm. The emulsion was liquefied under safelight (Kindermann GmbH, Ochsenfurt, Germany) in a water bath at +40°C. Slides were dipped into the liquid emulsion and then placed in a tilted position on a sucking underlay to remove surplus emulsion. Afterward, slides were placed briefly onto an ice-cooled metallic plate to harden the emulsion layer and then dried overnight in a lightproof box containing silica gel as a desiccant. The coated slides were stored until use in a black lightproof staining tray (Carl Roth GmbH and Co KG, Karlsruhe, Germany), also containing a desiccant.

Staining Solution. Stock solutions of methylene blue (0.640 g/500 ml of demineralized water) and basic fuchsin (0.648 g/500 ml of demineralized water) were produced. To 70 ml of 0.2 mol/l phosphate buffer (pH 7.2), 50 ml of absolute ethanol, 50 ml of methylene blue stock solution, and 50 ml of basic fuchsin stock solution were added to obtain the final methylene blue-basic fuchsin stain. The final methylene blue-basic fuchsin solution was filtered before each use.

Animals. Male albino rats of strain Crl:WI(Han) with a body weight of 164 to 184 g were supplied by Charles River Laboratories (Sulzfeld, Germany). The animals were fasted for approximately 20 h before dosing until 3 h after dosing. Drinking water was offered ad libitum. The rats were kept individually in cages under standardized environmental conditions. All animal procedures were conducted according to the ethical guidelines of the German Animal Welfare Act.

Study Conduct. Microscopic autoradiography was performed in an manner analogous to the method described by Stumpf (2003). [^{3}H]Linagliptin was used either unblended (7.4 μg/kg) or blended with nonlabeled linagliptin (100 and 2000 μg/kg) and dissolved in physiological saline. In addition, 4 g/kg of freshly prepared formulation was injected as a single bolus into a tail vein of the rats. Three rats received 7.4 μg/kg, and one rat each received 0 (control), 100, or 2000 μg/kg [^{3}H]linagliptin (Table 1). The rats dosed with 7.4 μg/kg were sacrificed at 2 min, 3 h, or 192 h after dosing; the other rats were sacrificed at 3 h after dosing. In parallel to the sample processing, photographic processing and staining of each tissue sample from [^{3}H]linagliptin-treated rats, a respective tissue sample from the control rat was handled.

Sample Processing. The kidney, liver, and small intestine (0 and 7.4 μg/kg) or just kidney (100 and 2000 μg/kg) were removed quickly and stored in an ice-cooled Petri dish until freeze mounting. Kidneys were dissected in two parts, a lobe of the liver, and a part of the jejunum were dissected. The prepared tissue samples were freeze-mounted with aqueous carboxymethyl cellulose (3–4%; w/v) on aluminum tissue holders (Leica Microsystems, Wetzlar, Germany). Thereafter the samples were frozen in isopentane that had been cooled by liquid nitrogen. Frozen specimens were transferred rapidly into liquid nitrogen and stored until sectioning in a cryostorage system (tec-lab GmbH, Idstein, Germany) at approximately −174°C. The frozen tissue samples were transferred in liquid nitrogen into the cryostat, in which the temperature of the specimen holder and cryochamber was set to between −21 and −23°C. After adjustment of the sample position, sectioning was performed with a cryomicrotome CM 3050S (Leica Microsystems). The samples were trimmed to the level of interest. Then the tissue sections, with a thickness of 5 μm, were produced under cold light illumination with a photo-optic lamp. In general, three sections were made for each slide. Under safelight conditions, an emulsion-coated slide was removed from the desiccator box outside of the cryostat at room temperature. The sections were picked up (thaw-mounted) through a quick and gentle touch of the pressure plate with the slide, avoiding pressure and hesitation. The section-mounted slide was then returned to the lightproof desiccator slide box and stored there at −24°C for up to 49 days. For exposition, the section-mounted slides in the boxes were stored in a refrigerator until development.

TABLE 1

Study design

Dose	Animal No.	Time Point of Investigation	Tissues Investigated
μg/kg			
0		Blank	Kidney, liver, small intestine
7.4	2	2 min	Kidney, liver, small intestine
7.4	3	3 h	Kidney, liver, small intestine
7.4	4	192 h	Kidney, liver, small intestine
100	5	3 h	Kidney
2000	6	3 h	Kidney

Photographic Processing and Staining. The exposure time under safelight conditions was determined empirically. Some hours before the end of the exposure time, the black box with the exposed slides was removed from the refrigerator or freezer and allowed to warm up to room temperature. At each time point, nonlabeled sections (animal 1) were also developed as a control. The slides were positioned in a slide carrier. After 4 min in a developer solution (D-19; Eastman Kodak Company, Rochester, NY), slides were quickly rinsed with tap water and fixed for approximately 8 min in a fixation solution (T-Max; Kodak Industrie, Chalon, France). Afterward, slides were rinsed with tap water for approximately 10 min. The wet slides were stained with methylene blue-basic fuchsin for 1 to 2 min. To remove excess stain from the sections and emulsion, slides were briefly washed in tap water. The stained slides were air-dried and then covered with a cover glass using DePeX (Serva, Heidelberg, Germany). Methylene blue-basic fuchsin staining renders nuclei blue, cytoplasm pink, and glycoprotein granules deep red.

Evaluation of Autoradiograms and Histology. With 5-μm thaw-mounted sections, both the structural and autoradiographic image can be viewed simultaneously in the same optical plane of the microscope (BX 61; Olympus GmbH, Hamburg, Germany), conveniently up to 400-fold magnification. With a high-sensitivity digital camera (CC-12; Olympus Soft Imaging Solutions GmbH, Münster, Germany) on top of the microscope in combination with a software tool (analySIS; Olympus Soft Imaging Solutions GmbH), images were produced and processed.

Results

The distribution of radioactivity in the kidney was investigated by dependence on dose, i.e., 3 h after intravenous bolus injection of 7.4, 100, and 2000 μg/kg [^{3}H]linagliptin. In addition, the distribution of radioactivity in the kidney, liver, and small intestine was investigated in relation to time, i.e., 2 min, 3 h, and 192 h after intravenous injection of 7.4 μg/kg [^{3}H]linagliptin.

Kidney. *Dose dependence at 3 h after dosing.* At 3 h after administration of 7.4 μg/kg relevant concentrations of radioactivity were revealed in the cortical proximal tubules. In addition, a remarkably high concentration of radioactivity was found in the glomeruli (Fig. 1). In the lower part of the proximal tubules (outer stripe of outer medulla) and distal parts of the nephron, almost no radioactivity was detectable. By 3 h after administration of 100 μg/kg, the bulk of radioactivity was located in the whole proximal tubules of the nephrons. Distinctly less radioactivity was visible in the glomeruli. In the distal parts of the nephron, only traces of radioactivity were detectable (Fig. 2). At 3 h after administration of 2000 μg/kg, only traces of radioactivity were visible in the glomeruli, the proximal convoluted tubules and in the distal part the nephrons. The bulk of radioactivity could be observed in the medullary rays containing a great number of straight proximal tubules (pars recta) (Fig. 3). Thus, the distribution pattern in the kidney at 3 h after intravenous bolus administration of [^{3}H]linagliptin was dose-dependent, i.e., different patterns were observed at 7.4, 100, or 2000 μg/kg with a shift from the glomeruli, dominating at 7.4 μg/kg, to the medullary rays containing a great number of straight proximal tubules dominating at 2000 μg/kg.

Time dependence at 7.4 μg/kg. At 2 min after administration of 7.4 μg/kg, a remarkably high concentration of radioactivity was found in the glomeruli of the kidney (Fig. 4). The distribution within the glomeruli exhibited a net-like structure. Only a moderate concentration of radioactivity was indicated in the upper part of the proximal tubules, whereas the lower part of the proximal tubules and the distal part of the nephron (Henle's loops, distal tubules, and collecting tubes) contained almost no radioactivity. Within the proximal tubules, the radioactivity appeared to be located primarily in the brush border

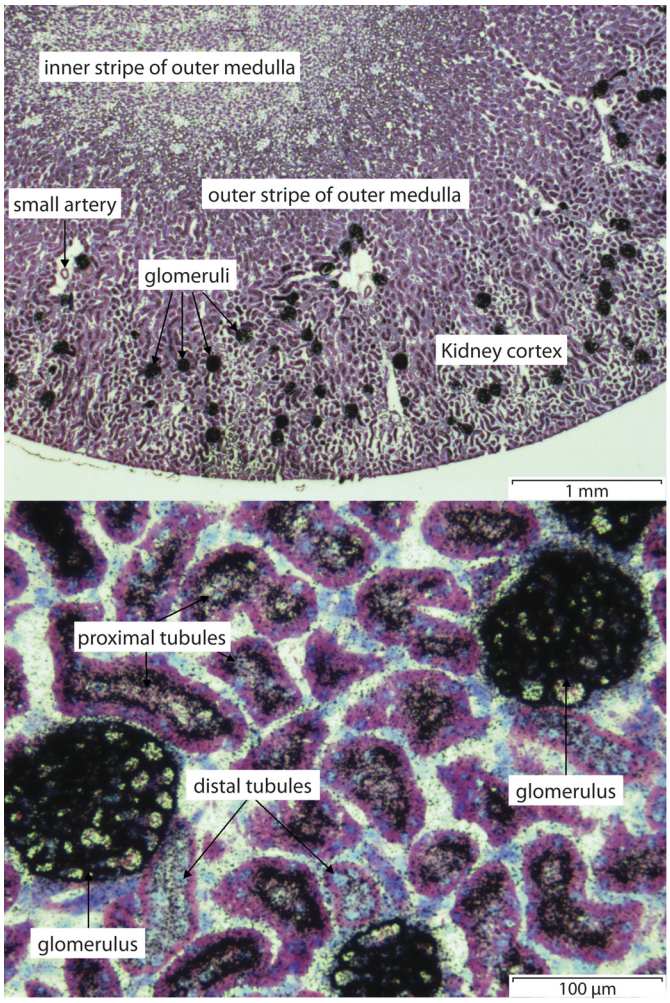

FIG. 1. Microautoradiograms from rat kidney sampled at 3 h after intravenous injection of 7.4 µg/kg [^{3}H]linagliptin.

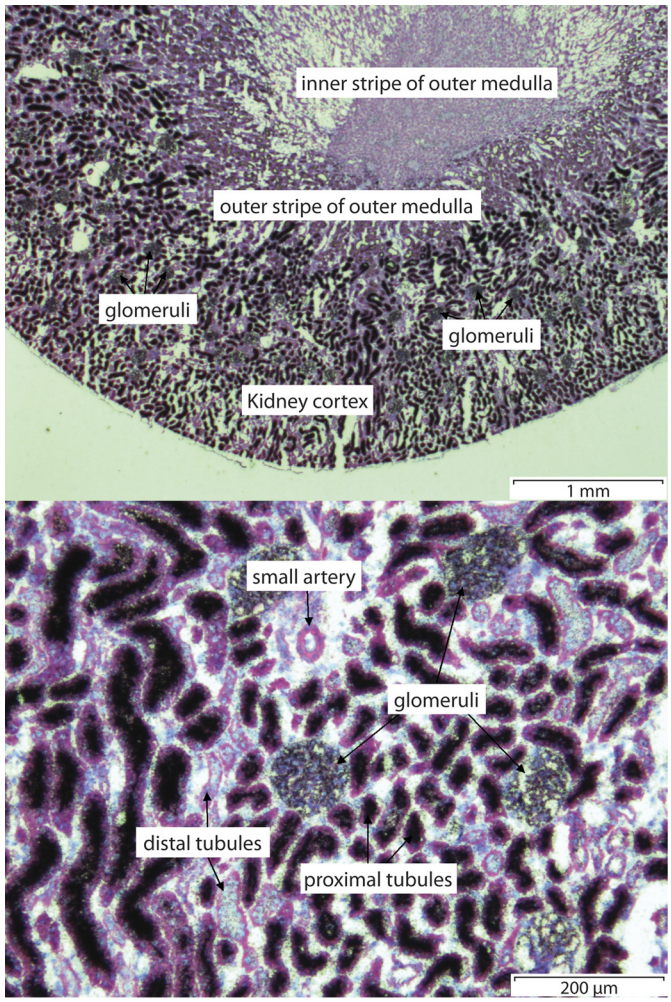

FIG. 2. Microautoradiograms from rat kidney sampled at 3 h after intravenous injection of 100 µg/kg [^{3}H]linagliptin.

of the tubular cells. As described above, 3 h after administration of 7.4 µg/kg, distinctly more radioactivity occurred in the cortical proximal tubules. The remarkably high concentration of radioactivity in the glomeruli of the kidney persisted (Fig. 1). At 192 h after administration of 7.4 µg/kg, the radioactivity was concentrated in the convoluted (upper) and rectal (lower) parts of the proximal tubules of the nephrons (outer stripe of outer medulla). In the glomeruli, only slight radioactivity remained, whereas in the distal parts of the nephron nearly no radioactivity was located (Fig. 5). Thus, the qualitative distribution pattern of the radioactivity in rat kidney changed with time after intravenous bolus administration of 7.4 µg/kg [^{3}H]linagliptin, as the maximum concentration of radioactivity shifted along the nephron from glomeruli (2 min) to the upper part (3 h) and lower part (192 h) of the proximal tubules.

Liver. At 2 min after administration of 7.4 µg/kg, a retiform distribution was observed in the liver, caused by a distinct higher concentration of the radioactivity located in the acinus zone 1 of liver around the portal triads and weakly in the bile duct (Fig. 6). At 3 h after administration of 7.4 µg/kg in the liver, the qualitative distribution pattern in the liver was nearly unchanged (data not shown). At 192 h after administration of 7.4 µg/kg, the retiform distribution of radioactivity was still visible. The concentration in the acinus of liver and the portal triads seems to be decreased, whereas the concentration of radioactivity in the other hepatocytes apparently persisted (Fig. 6). The radioactivity was also prominent on the intraluminal surface of the bile duct. Thus, a distinctive retiform distribution of the radioactivity was observed in the liver after intravenous bolus administration of 7.4 µg/kg [^{3}H]linagliptin, which reduced in intensity with time.

Small Intestine. At 2 min after administration of 7.4 µg/kg, the radioactivity in the small intestine was located primarily in the lamina propria and secondarily on the surface of the villi and/or in the lumen, whereas in the submucosa slightly less radioactivity was found (Fig. 7). At 3 h after administration of 7.4 µg/kg, the bulk of the radioactivity was located on the surface of the villi and/or in the lumen of the small intestine (Fig. 7). At 192 h after administration of 7.4 µg/kg, only traces of radioactivity were detectable on the surface of the villi of the small intestine. In addition, traces of radioactivity were visible in the connective tissue layer between the pancreas and small intestine (data not shown). Thus, a shift of the radioactivity in the small intestine with time from the lamina propria, (dominant at 2 min) to the surface of the villi and/or lumen (dominant at 3 and 192 h) was indicated after intravenous bolus administration of 7.4 µg/kg [^{3}H]linagliptin.

Discussion

Linagliptin is unusual within the DPP-4 class in that it shows target-mediated nonlinear pharmacokinetics and a lack of relevant renal excretion (Retlich et al., 2009; Deacon and Holst, 2010). The current study examined the dose and time dependence of distribution of linagliptin-related radioactivity within the excretory organs kidney,

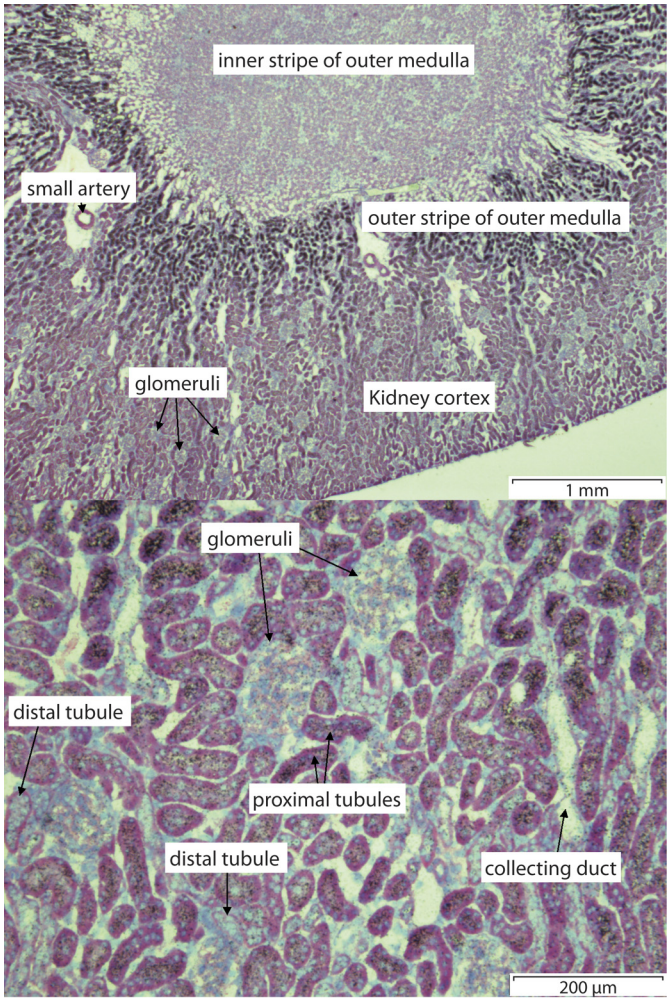

FIG. 3. Microautoradiograms from rat kidney sampled at 3 h after intravenous injection of 2000 μg/kg [^{3}H]linagliptin.

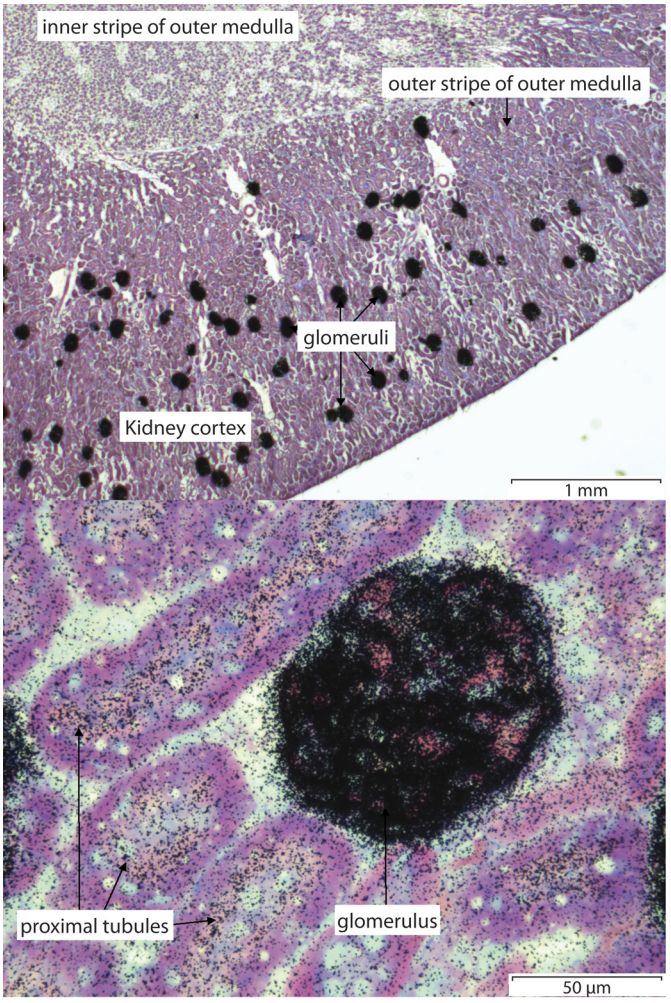

FIG. 4. Microautoradiograms from rat kidney sampled at 2 min after intravenous injection of 7.4 μg/kg [^{3}H]linagliptin.

liver, and small intestine, in which DPP-4 is known to be expressed at high levels. The gross distribution pattern of radioactivity in the kidney after administration of 2000 μg/kg [^{3}H]linagliptin observed in this study using microscopic autoradiography was very similar to the respective pattern obtained in a previous study using classic whole-body autoradiography after intravenous dosing of 2000 μg/kg [^{14}C]linagliptin (Fuchs et al., 2009a). Thus, the results obtained with this technique are assessed as validated and reflect the in vivo distribution pattern of [^{3}H]linagliptin-related radioactivity adequately and with higher resolution on a cellular level. Because the radioactivity levels in the kidney and liver after dosing of radiolabeled linagliptin can be primarily assigned to a parent drug (Fuchs et al., 2009a), the distribution patterns are assumed to be the distribution patterns of linagliptin itself. In addition, it was shown that the persistent binding can be attributed to binding to DPP-4 (Fuchs et al., 2009a).

The distribution of linagliptin into kidney was noticeably dose-dependent, as shown previously (Fuchs et al., 2009a). This dose effect was investigated on a cellular level within the kidney in the current study. By 3 h after dosing of 7.4 μg/kg, radioactivity was detected primarily in the glomeruli, showing a retiform distribution pattern. In contrast, 3 h after dosing of 100 μg/kg the radioactivity was primarily found in the brush border of the cortical convoluted proximal tubules, and 3 h after dosing of 2000 μg/kg the bulk of radioactivity was observed in the medullary rays containing a great number of proximal straight tubules (pars recta). Thus, the focus of radioactivity distribution was shifted with increasing dose from the glomeruli over the cortical convoluted proximal tubules to the straight proximal tubules (outer stripe of outer medulla). This may be the result of a saturation of binding sites for linagliptin: i.e., at the low dose, the radioactivity might be trapped by the glomeruli, exhibiting low binding capacity; at the mid-dose the radioactivity spilled over with the primary urine to the upper part of the proximal tubules, exhibiting moderate binding capacity; and at the high dose the radioactivity further spilled over to the lower part of the proximal tubules, exhibiting high binding capacity. Less radioactivity was found in the distal tubules, which seem to have no binding sites. It has to be noted that the proportion of labeled to nonlabeled linagliptin changed with dosage, which resulted in different limits of detection. Thus, a drug concentration resulting in radiostaining of a tissue at the low dose might not have stained the same tissue at the high dose. On the other hand, the high specific radioactivity of the labeled linagliptin of up to 3 MBq/nmol allowed the use of low doses and thus enabled us to differentiate between specific (target) and nonspecific binding. Overall, however, the tissue distribution pattern of radioactivity in the kidney after dosing of the DPP-4 inhibitor [^{3}H]linagliptin was similar to the tissue distribution pattern of DPP-4, which is described to be located on glomerular podocytes (fitting to the observed retiform distribution of radioactivity in the glomeruli) and on the brush border microvilli of the proximal tubules (Hartel et al., 1988a; Hong et al., 1989; Hartel-Schenk et al., 1990; Kettmann et al., 1992; Lambeir et al., 2003). In addition to the

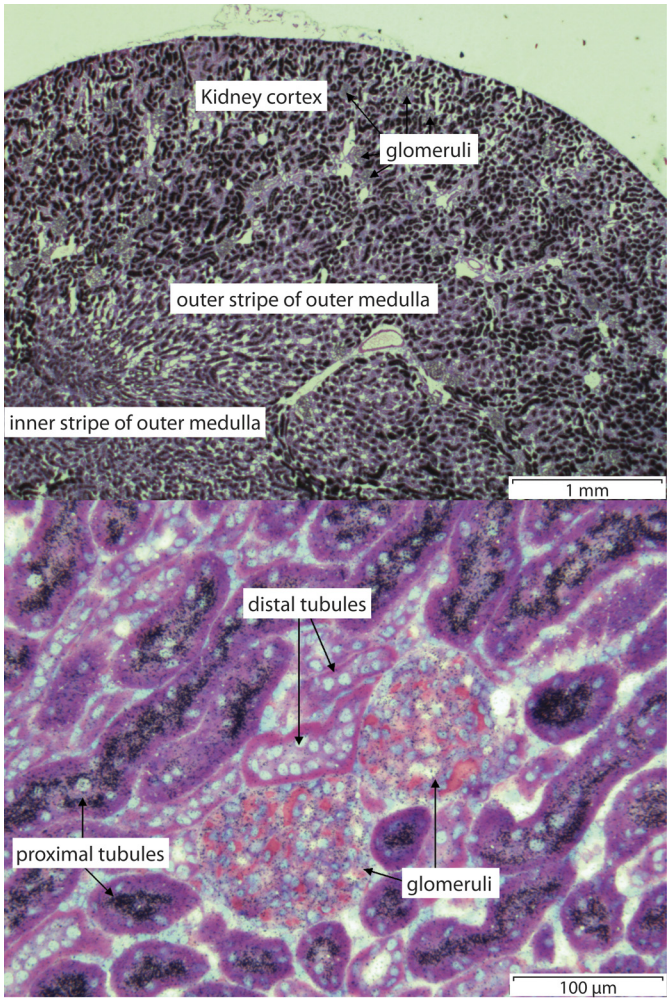

FIG. 5. Microautoradiograms from rat kidney sampled at 192 h after intravenous injection of 7.4 µg/kg [^{3}H]linagliptin.

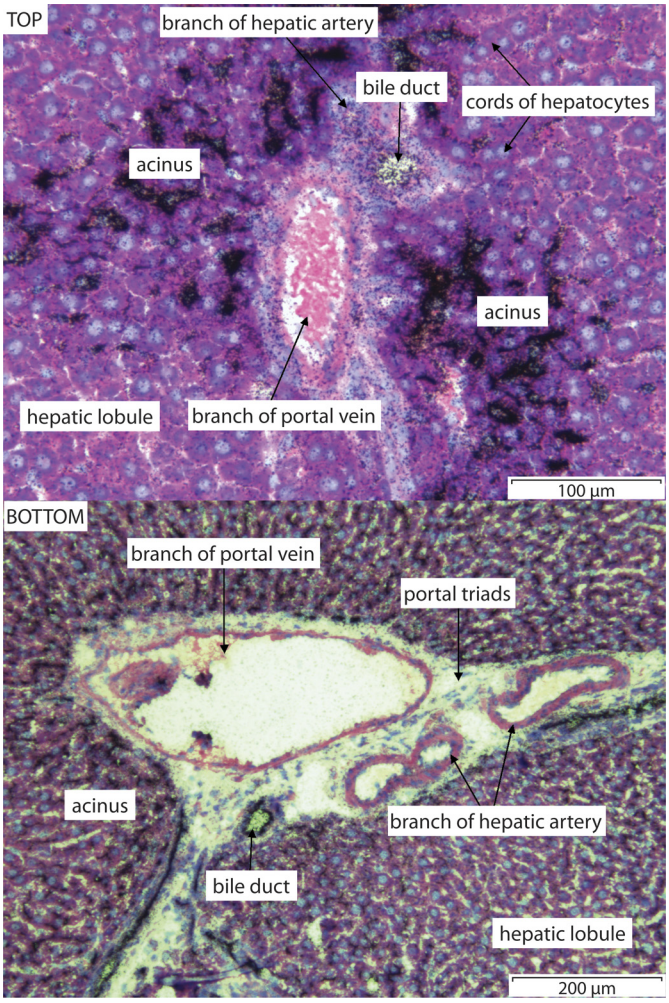

FIG. 6. Microautoradiograms from rat liver sampled at 2 min (top) or 192 h (bottom) after intravenous injection of 7.4 µg/kg [^{3}H]linagliptin.

dose dependence of the distribution pattern of radioactivity, a prominent time dependence of the distribution pattern of radioactivity in the kidney was observed after dosing of 7.4 µg/kg [^{3}H]linagliptin, because the maximum concentration of radioactivity shifted along the nephron from the glomeruli (2 min) to the upper (3 h) and lower part (192 h) of the proximal tubules. It has to be noted that almost no time dependence was observed in the radioactive pattern of the kidney after dosing of 2000 µg/kg (J. Baierl, R. Binder, and A. Greischel, unpublished data) but only at low doses, indicating that the time effect depends on unsaturated binding sites. Thus, the time dependence might be caused by the reversible nature of bound radioactive material in the glomeruli and passage through the nephron: the radioactivity arriving in the kidney might be trapped by low-capacity binding sites in the glomeruli and then washed out with the primary urine into the convoluted proximal tubules, where most of the filtrated water is reabsorbed and sufficient binding sites are available, and then further washed down into the lower part of the proximal tubules. An additional secretion via transporters into the convoluted proximal tubules cannot be excluded.

In the liver, a retiform distribution was observed at 2 min, 3 h, and 196 h after dosing of 7.4 µg/kg, which is a result of high concentrations of radioactivity in the acinus zone 1 around the portal triads. The pattern was observed at all time points but was reduced in intensity with time. The long persistence of the radioactive pattern indicates a strong binding. Because DPP-4 is abundant on the epithelial cells of the bile duct and on the hepatocytes around the bile canaliculi, the observed pattern of radioactivity in the liver might reflect binding of [^{3}H]linagliptin to DPP-4 (Hartel et al., 1988b; Hong et al., 1989; Lambeir et al., 2003).

In the small intestine, a nonuniform and time-dependent distribution of radioactivity was observed after dosing of 7.4 µg/kg. At 2 min after administration, the radioactivity was located primarily in the lamina propria, 3 h after administration the bulk of radioactivity was now located on the surface of the villi and/or in the lumen of the small intestine, and at 192 h after administration only traces of radioactivity were detectable on the surface of the villi and/or in the lumen of the small intestine. Thus, there was a shift of the radioactivity with time from the lamina propria to the surface of the villi or even directly into the lumen. This distribution pattern fits with the published expression pattern of DPP-4 in the capillaries of the lamina propria and on the brush border membranes of the small intestine (Hartel-Schenk et al., 1990; Hansen et al., 1999; Lambeir et al., 2003). However, the pictures did not substantiate binding to these structures in the small intestine, and the distribution pattern and time dependence might also be caused by secretion of linagliptin into the intestinal lumen, e.g., by P-glycoprotein, as linagliptin was shown to be a P-glycoprotein substrate (T. Flötotto, unpublished results).

Overall the distribution patterns of linagliptin in the kidney, liver, and small intestine were shown to be significantly influenced by highly specific and reversible binding of linagliptin to DPP-4 and less

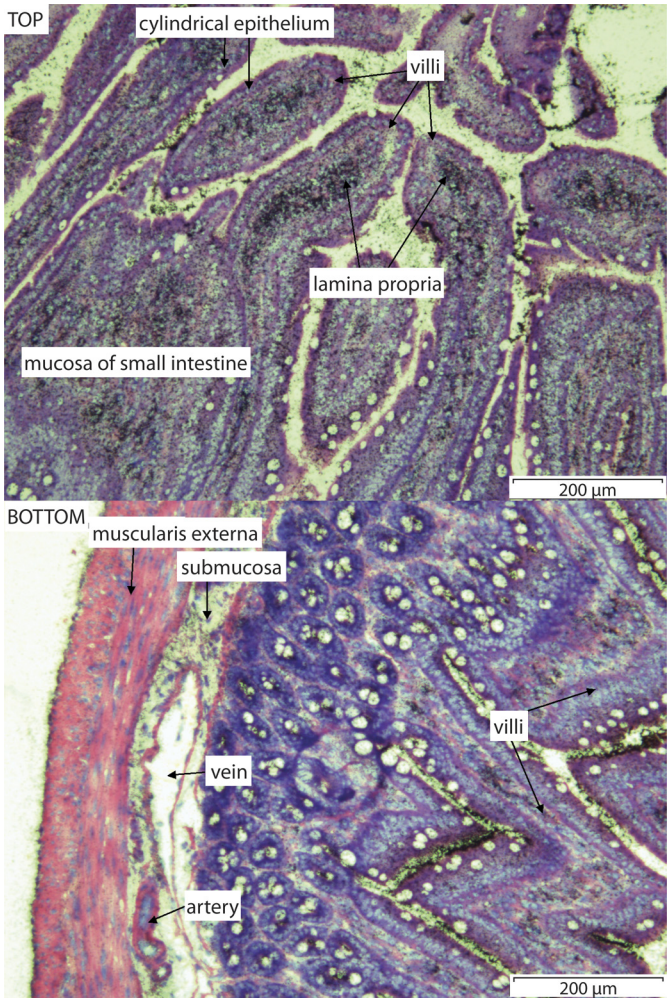

FIG. 7. Microautoradiograms from rat small intestine sampled at 2 min (top) or 3 h (bottom) after intravenous injection of 7.4 μg/kg [^{3}H]linagliptin.

by nonspecific binding. Similar distribution behavior can be expected in humans, because the therapeutic dose of linagliptin is low and the DPP-4 expression pattern in tissues is similar in rats and humans. In general, the distribution pattern of [^{3}H]linagliptin-related radioactivity on a cellular level in the kidney, liver, and intestine of rats closely resembled the known distribution of DPP-4. The distribution pattern in the kidney was shown to be both time- and dose-dependent, which is indicated to be caused by saturation of highly specific and reversible binding of linagliptin to DPP-4 in the glomeruli and especially proximal tubules. A similar effect can be expected in humans, as the therapeutic dose of linagliptin is low and DPP-4 is also expressed in the human kidney.

Acknowledgments. We thank Dr. Florian Colbatzky for his histological review and Dr. Holger Fuchs for helpful discussions. Editorial support (language assistance and proofreading) for the article was provided by Richard Ogilvy-Stewart, Ph.D., of PHASE II International Ltd.

References

Deacon CF and Holst JJ (2010) Linagliptin, a xanthine-based dipeptidyl peptidase-4 inhibitor with an unusual profile for the treatment of type 2 diabetes. *Expert Opin Investig Drugs* **19:**133–140.

Eckhardt M, Hauel N, Himmelsbach F, Langkopf E, Nar H, Mark M, Tadayyon M, Thomas L, Guth B, and Lotz R (2008) 3,5-Dihydro-imidazol[4,5 days]pyridazin-4-ones: a class of potent DPP-4 inhibitors. *Bioorg Med Chem Lett* **18:**3158–3162.

Fuchs H, Binder R, and Greischel A (2009a) Tissue distribution of the novel DPP-4 inhibitor BI 1356 is dominated by saturable binding to its target in rats. *Biopharm Drug Dispos* **30:**229–240.

Fuchs H, Tillement JP, Urien S, Greischel A, and Roth W (2009b) Concentration-dependent plasma protein binding of the novel dipeptidyl peptidase 4 inhibitor BI 1356 due to saturable binding to its target in plasma of mice, rats and humans. *J Pharm Pharmacol* **61:**55–62.

Fukasawa KM, Fukasawa K, Sahara N, Harada M, Kondo Y, and Nagatsu I (1981) Immunohistochemical localization of dipeptidyl aminopeptidase IV in rat kidney, liver, and salivary glands. *J Histochem Cytochem* **29:**337–343.

Hansen L, Deacon CF, Orskov C, and Holst JJ (1999) Glucagon-like peptide-1-(7–36)amide is transformed to glucagon-like peptide-1-(9–36)amide by dipeptidyl peptidase IV in the capillaries supplying the L cells of porcine intestine. *Endocrinology* **140:**5356–5363.

Hartel S, Gossrau R, Hanski C, and Reutter W (1988a) Dipeptidyl peptidase (DPP) IV in rat organs. Comparison of immunohistochemistry and activity histochemistry. *Histochemistry* **89:**151–161.

Hartel S, Hanski C, Neumeier R, Gossrau R, and Reutter W (1988b) Characterization of different forms of dipeptidyl peptidase IV from rat liver and hepatoma by monoclonal antibodies. *Adv Exp Med Biol* **240:**207–214.

Hartel-Schenk S, Gossrau R, and Reutter W (1990) Comparative immunohistochemistry and histochemistry of dipeptidyl peptidase IV in rat organs during development. *Histochem J* **22:**567–578.

Heise T, Graefe-Mody EU, Hüttner S, Ring A, Trommeshauser D, and Dugi KA (2009) Pharmacokinetics, pharmacodynamics and tolerability of multiple oral doses of linagliptin, a dipeptidyl peptidase-4 inhibitor in male type 2 diabetes patients. *Diabetes Obes Metab* **11:**786–794.

Hong WJ, Petell JK, Swank D, Sanford J, Hixson DC, and Doyle D (1989) Expression of dipeptidyl peptidase IV in rat tissues is mainly regulated at the mRNA levels. *Exp Cell Res* **182:**256–266.

Kettmann U, Humbel B, and Holzhausen HJ (1992) Ultrastructural localization of dipeptidylpeptidase IV in the glomerulum of the rat kidney. *Acta Histochem* **92:**225–227.

Lambeir AM, Durinx C, Scharpé S, and De Meester I (2003) Dipeptidyl-peptidase IV from bench to bedside: an update on structural properties, functions, and clinical aspects of the enzyme DPP IV. *Crit Rev Clin Lab Sci* **40:**209–294.

Mentlein R (1999) Dipeptidyl-peptidase IV (CD26)—role in the inactivation of regulatory peptides. *Regul Pept* **85:**9–24.

Retlich S, Withopf B, Greischel A, Staab A, Jaehde U, and Fuchs H (2009) Binding to dipeptidyl peptidase-4 determines the disposition of linagliptin (BI 1356)—investigations in DPP-4 deficient and wildtype rats. *Biopharm Drug Dispos* **30:**422–436.

Stumpf WE (2003) Drug localization in tissues and cells. Receptor microscopic autoradiography. A basis for tissue and cellular pharmacokinetics, drug targeting, delivery and prediction, in *International Institute of Drug Distribution, Cytopharmacology and Cytotoxicology*, IDDC Press, Chapel Hill, NC.

Address correspondence to: Dr. Andreas Greischel, Drug Metabolism and Pharmacokinetics, Boehringer Ingelheim GmbH & Co. KG, Birkendorfer Str. 65, D-88397 Biberach an der Riss, Germany. E-mail: andreas.greischel@boehringer-ingelheim.com